

Chiral Terminal Platinum(II) Phosphido Complexes: Synthesis, Phosphorus Inversion, and Acrylonitrile Insertion

Denyce K. Wicht, Ivan Kovacic, and David S. Glueck*

Department of Chemistry, Dartmouth College, 6128 Burke Laboratory,
Hanover, New Hampshire 03755

Louise M. Liable-Sands, Christopher D. Incarvito, and Arnold L. Rheingold

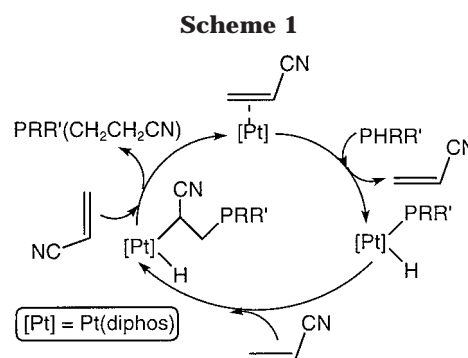
Department of Chemistry, University of Delaware, Newark, Delaware 19716

Received May 18, 1999

The chiral Pt(II) phosphido complex $\text{Pt}(\text{dppe})(\text{Me})[\text{P}(\text{Mes})(\text{Men})]$ ($\text{dppe} = \text{Ph}_2\text{PCH}_2\text{CH}_2\text{PPh}_2$, $\text{Mes} = 2,4,6\text{-Me}_3\text{C}_6\text{H}_2$, $\text{Men} = (-)\text{menthyl}$, **1**) was prepared by proton transfer from racemic mesityl(-)menthylphosphine to the methoxide ligand of $\text{Pt}(\text{dppe})(\text{Me})(\text{OMe})$. Treatment of $\text{Pt}(\text{dcpe})[\text{CH}(\text{Me})(\text{CN})](\text{Br})$ with alkali metal phosphides gives $\text{Pt}(\text{dcpe})[\text{CH}(\text{Me})(\text{CN})](\text{PRR}')$ ($\text{dcpe} = \text{Cy}_2\text{PCH}_2\text{CH}_2\text{PCy}_2$, $\text{Cy} = \text{cyclo-C}_6\text{H}_{11}$, $\text{R} = \text{H}$, $\text{R}' = \text{Mes}^* = 2,4,6\text{-}(t\text{-Bu})_3\text{C}_6\text{H}_2$, **13**; $\text{R} = \text{Me}$, $\text{R}' = \text{Ph}$, **14**). The related series of complexes $\text{Pt}(\text{diphos}^*)(\text{Me})(\text{PRR}')$ ($\text{diphos}^* = S,S\text{-Chiraphos}$, $\text{R} = \text{Ph}$, $\text{R}' = \text{Is} = 2,4,6\text{-}(i\text{-Pr})_3\text{C}_6\text{H}_2$, **5**; $\text{R} = \text{Me}$, $\text{R}' = \text{Mes}^*$, **6**; $\text{diphos}^* = R\text{-Tol-Binap}$, $\text{R} = \text{Me}$, $\text{R}' = \text{Mes}^*$, **7**) containing chiral diphosphine ligands has been prepared by deprotonation of the cations $[\text{Pt}(\text{diphos}^*)(\text{Me})(\text{PHRR}')][\text{BF}_4]$ **2**, **3**, and **4**, respectively. The cations, synthesized from $\text{Pt}(\text{diphos}^*)(\text{Me})(\text{Cl})$, AgBF_4 , and the appropriate secondary phosphine, were isolated as a mixture of diastereomers (**2** and **3**) or a single isomer (**4**). Phosphido complexes **1** and **5–7** show only one set of ^{31}P NMR resonances in solution even at low temperature, consistent either with the existence of a single diastereomer or with rapid inversion at phosphorus. However, low-temperature spectra of **13** and **14** reveal the existence of the expected two diastereomers, which interconvert by phosphorus inversion and rotation about the Pt–P bond with barriers of approximately 11.5 and 15.5 kcal/mol, respectively. Treatment of **6** and **7** with HBF_4 protonates the phosphido ligand and generates diastereomeric mixtures of the cations **3** and **4**, respectively. Acrylonitrile inserts into the Pt–P bond of **1** to give the dialkyl complex $\text{Pt}(\text{dppe})(\text{Me})[\text{CH}(\text{CN})\text{CH}_2\text{P}(\text{Mes})(\text{Men})]$ (**9**) as a mixture of four diastereomers; similar product mixtures (**10–12**) are obtained with **5–7**. Complexes $4 \cdot 3\text{CH}_2\text{Cl}_2$, **5**, and the secondary phosphine $\text{PH}(\text{Me})(\text{Mes}^*)$ (**8**) were structurally characterized by X-ray crystallography.

Introduction

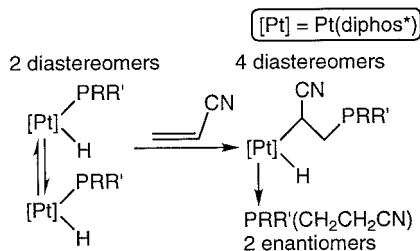
Recently, we have provided evidence that P–C bond formation in Pt-catalyzed hydrophosphination of acrylonitrile occurs by insertion of the olefin into a Pt–phosphido bond (Scheme 1).¹ The model compounds $\text{M}(\text{dppe})(\text{Me})(\text{PHMes}^*)$ ($\text{M} = \text{Pd}, \text{Pt}$; $\text{Mes}^* = 2,4,6\text{-}(t\text{-Bu})_3\text{C}_6\text{H}_2$) undergo selective insertion to afford $\text{M}(\text{dppe})(\text{Me})[\text{CH}(\text{CN})\text{CH}_2\text{PHMes}^*]$ as a mixture of diastereomers in about a 2:1 ratio. This observation suggests that a chiral Pt(diphos^*) fragment ($\text{diphos}^* = \text{chiral diphosphine}$) might catalyze asymmetric hydrophosphination of secondary phosphines PHRR' to give enantio-enriched tertiary phosphines $\text{PRR}'(\text{CH}_2\text{CH}_2\text{CN})$ (Scheme 2). In this case, oxidative addition of racemic PHRR' would give a phosphido hydride intermediate $\text{Pt}(\text{diphos}^*)(\text{PRR}')(\text{H})$ as a mixture of diastereomers. Since barriers to pyramidal inversion in transition metal



phosphido complexes are low,² these isomers should interconvert readily by inversion at phosphorus.³ If one is energetically favored, then two of the four possible alkyl hydride diastereomers would be formed preferentially on acrylonitrile insertion, and reductive elimination would yield preferentially one enantiomer of the configurationally stable⁴ tertiary phosphine $\text{PRR}'(\text{CH}_2\text{CH}_2\text{CN})$ via thermodynamic resolution.⁵ Alternatively, the phosphido hydride diastereomers might interconvert

(1) (a) Wicht, D. K.; Kourkine, I. V.; Lew, B. M.; Nthenge, J. M.; Glueck, D. S. *J. Am. Chem. Soc.* **1997**, *119*, 5039–5040. (b) Wicht, D. K.; Kourkine, I. V.; Kovacic, I.; Glueck, D. S.; Concolino, T.; Yap, G. P. A.; Incarvito, C. D.; Rheingold, A. L. *Organometallics*, accepted for publication.

Scheme 2



more quickly than they react with acrylonitrile; if one reacts faster than the other, then enantio-enriched product could be formed via dynamic kinetic resolution.⁶

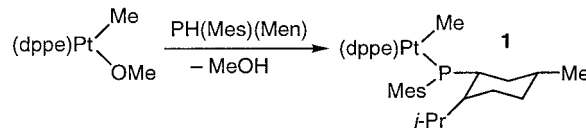
To investigate these possibilities, we report here studies of phosphorus inversion in model chiral Pt(II) phosphido complexes and of the diastereoselectivity of acrylonitrile insertion in these compounds.

Results and Discussion

We studied three types of Pt(diphos)(R)(PR'R'') complexes: one has a chiral phosphido substituent, another contains a chiral diphos ligand, and a third includes a chiral Pt-bound alkyl group. If phosphorus inversion is slow on the NMR time scale, the NMR spectra should exhibit signals due to both expected diastereomers, as long as one diastereomer is not much higher in energy than the other. For example, the iron-phosphido complex (*R,R*)-Fe(Cp){1,2-C₆H₄(PMePh)₂}(PPh)₂^{2c} exists at -65 °C as a 4.5:1 mixture of diastereomers, as shown by the observation of two different Cp resonances in the ¹H NMR spectrum. As the temperature is raised, these signals coalesce; from the ¹H NMR data, the barrier to pyramidal inversion at phosphorus was reported to be 60 kJ mol⁻¹.

The complex Pt(dppe)(Me)[P(Mes)(Men)] (Mes = 2,4,6-Me₃C₆H₂, Men = (-)-menthyl, **1**) was prepared from racemic mesitylmenthylphosphine^{3a} and Pt(dppe)(Me)(OMe) (Scheme 3), as reported for a variety of other secondary phosphines.⁷ The room-temperature ³¹P{¹H} NMR spectrum of **1** (toluene-*d*₈; see Table 1 for ³¹P NMR

Scheme 3



data for this and other compounds) contains sharp dppe resonances and a broad phosphido signal. At -75 °C, the phosphido peak is sharp, while the dppe signals undergo small changes in chemical shift and coupling constants. A similar spectrum is observed at 80 °C, although the phosphido resonance is still rather broad. While these observations are consistent with the proposed structure for **1**, they are ambiguous about the possible inversion process. We assume that the unusual broadness of signals due to the cis dppe and phosphido P nuclei is due to a dynamic process involving rotation about the Pt-P(Mes)(Men) bond, which affects the environment of the neighboring cis dppe group. This interpretation is supported by similar observations in related complexes (see **5** below and the preceding article.)⁸

At 21 °C in toluene-*d*₈, the ¹H NMR spectrum of **1** shows only one set of signals for the Mes (δ 3.01, 6H; 2.11 (3H)) and Pt-Me (δ 0.88, m, *J*_{Pt-H} = 72 Hz, 3H) groups, as well as for the menthyl isopropyl and methyl groups. As the sample is cooled, the *o*-Me mesityl resonance broadens and finally decoalesces into two peaks (-75 °C) at δ 3.56 (3H) and 3.19 (3H), consistent with restricted rotation about the P-C(Mes) bond at this temperature. The other signals broaden but do not undergo other significant changes on cooling. From these data, we cannot tell if one diastereomer of complex **1** is so energetically favored that the other is not observed or if the two possible isomers are rapidly interconverting on the NMR time scale.

To prepare related phosphido complexes with chiral chelating diphosphine ligands, the cations [Pt(diphos*)(Me)(PHRR')][BF₄] (diphos* = *S,S*-Chiraphos; R = Ph, R' = Is = 2,4,6-(*i*-Pr)₃C₆H₂, **2**; R = Me, R' = Mes*, **3**; diphos* = *R-Tol-Binap*, R = Me, R' = Mes*, **4**, Scheme 4) were synthesized from Pt(diphos*)(Me)(Cl), a slight excess of the corresponding phosphine, and AgBF₄. Pt(*S,S*-Chiraphos)(Me)(Cl) was previously prepared by the addition of the diphosphine ligand to Pt(COD)(Me)(Cl);⁹ the new compound Pt(*R-Tol-Binap*)(Me)(Cl) was made in the same way (see the Experimental Section).

Since secondary phosphines racemize quickly, 1 equiv of a phosphine should give a thermodynamic mixture of diastereomers [Pt(diphos*)(Me)(PHRR')]⁺. For example, Wild^{3b} has reported that [Pt{1,2-C₆H₄(PMePh)₂}-{PH(Me)(Ph)}Cl]⁺ exists as a 2:1 mixture of isomers, one of which was isolated by fractional recrystallization. Similar results were observed for the cations **2** and **3**, which were obtained as mixtures of diastereomers (1:1 for **2**, 3:1 for **3**). Although **4** is initially formed as a 10:1 mixture of isomers, according to ³¹P NMR monitoring, stirring the reaction mixture at room temperature for

(2) For examples, see: (a) Buhro, W. E.; Gladysz, J. A. *Inorg. Chem.* **1985**, *24*, 3505-3507. (b) Simpson, R. D.; Bergman, R. G. *Organometallics* **1992**, *11*, 3980-3993. (c) Crisp, G. T.; Salem, G.; Wild, S. B.; Stephan, F. S. *Organometallics* **1989**, *8*, 2360-2367. (d) Malisch, W.; Maisch, R.; Meyer, A.; Greissinger, D.; Gross, E.; Colquhoun, E. J.; McFarlane, W. *Phosphorus Sulfur* **1983**, *18*, 299-302. (e) Baker, R. T.; Whitney, J. G.; Wreford, S. S. *Organometallics* **1983**, *2*, 1049-1051. (f) Bonnet, G.; Kubicki, M. M.; Moise, C.; Lazzaroni, R.; Salvadori, P.; Vitulli, G. *Organometallics* **1992**, *11*, 964-967. (g) Fryzuk, M. D.; Joshi, K.; Chadha, R. K.; Rettig, S. J. *J. Am. Chem. Soc.* **1991**, *113*, 8724-8736. (h) Malisch, W.; Gunzelmann, N.; Thirase, K.; Neumayer, M. *J. Organomet. Chem.* **1998**, *571*, 215-222. For a review, see: (i) Rogers, J. R.; Wagner, T. P. S.; Marynick, D. S. *Inorg. Chem.* **1994**, *33*, 3104-3110.

(3) Diastereoselectivity in the oxidative addition is also possible. Since secondary phosphines readily racemize in solution by acid- or base-catalyzed processes, dynamic resolution might also occur in this step. See: (a) Bader, A.; Pabel, M.; Wild, S. B. *J. Chem. Soc., Chem. Commun.* **1994**, 1405-1406. (b) Bader, A.; Nullmeyers, T.; Pabel, M.; Salem, G.; Willis, A. C.; Wild, S. B. *Inorg. Chem.* **1995**, *34*, 384-389.

(4) (a) Baechler, R. D.; Mislou, K. *J. Am. Chem. Soc.* **1970**, *92*, 3090. (b) Mislou, K. *Trans. N. Y. Acad. Sci.* **1973**, *35*, 227-242.

(5) (a) Beak, P.; Basu, A.; Gallagher, D. J.; Park, Y. S.; Thayumanavan, S. *Acc. Chem. Res.* **1996**, *29*, 552-560. (b) Vedejs, E.; Donde, Y. *J. Am. Chem. Soc.* **1997**, *119*, 9293-9294. (c) Wolfe, B.; Livinghouse, T. *J. Am. Chem. Soc.* **1998**, *120*, 5116-5117.

(6) (a) Ward, R. S. *Tetrahedron: Asymmetry* **1995**, *6*, 1475-1490. (b) Noyori, R.; Tokunaga, M.; Kitamura, M. *Bull. Chem. Soc. Jpn.* **1995**, *68*, 36-56. (c) Caddick, S.; Jenkins, K. *Chem. Soc. Rev.* **1996**, *25*, 447-456.

(7) Wicht, D. K.; Paisner, S. N.; Lew, B. M.; Glueck, D. S.; Yap, G. P. A.; Liable-Sands, L. M.; Rheingold, A. L.; Haar, C. M.; Nolan, S. P. *Organometallics* **1998**, *17*, 652-660.

(8) Wicht, D. K.; Glueck, D. S.; Liable-Sands, L. M.; Rheingold, A. L. *Organometallics* **1999**, *18*, 5130.

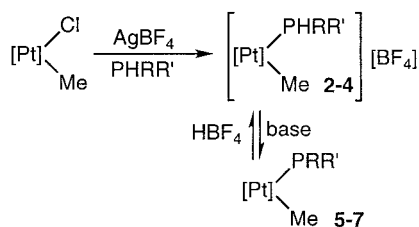
(9) Payne, N. C.; Stephan, D. W. *J. Organomet. Chem.* **1981**, *221*, 203-221.

Table 1. ^{31}P NMR Data for $[\text{Pt}(\text{diphos})(\text{R})(\text{X})]^{n+}$ (**1–7**, **13**, **14**)^{a–c}

diphos, R (No.)	X	$\delta(\text{P}_1)$ ($J_{\text{Pt-P}}$)	$\delta(\text{P}_2)$ ($J_{\text{Pt-P}}$)	$\delta(\text{P}_3)$ ($J_{\text{Pt-P}}$)	J_{12}	J_{13}	J_{23}
dppe, Me (1)	P(Mes)(Men)	48.2 (1782)	44.3	-16.5		166	
			(br, 1920)	(v br)			
		50.7 (1830)	49.2 (1920)	-9.4 (1115)		183	
		47.3 (1759)	42.3 (1917)	-21.7 (br, 1100)		159	
Chiraphos, Me (2a) ^d	PH(Ph)(Is)	51.3 (2814)	47.3 (1749)	-22.1 (2593)	17	375	18
		(2b)	51.2 (2813)	47.0 (1628)	-30.4 (2532)	17	385
Chiraphos, Me (3a) ^d	PH(Me)(Mes*)	49.5 (2773)	47.6 (1661)	-36.1 (2684)	17	384	14
		(3b)	52.7 (2805)	45.8 (1737)	-46.2 (2591)	16	395
Tol-Binap, Me	Cl	22.5 (1770)	16.6 (4395)		17		
Tol-Binap, Me (4a)	PH(Me)(Mes*)	22.0 (2986)	14.9 (1832)	-32.0 (2736)	23	410	20
		(4b) ^e	23.3	16.7	-41.4 (2646)	23	416
Chiraphos, Me (5)	P(Ph)(Is)	48.8 (1981)	48.2 (1904)	-21.0 (1126)	12	188	
Chiraphos, Me (6)	P(Me)(Mes*)	47.9 (1816)	51.0 (1932)	-13.1 (1176)	11	171	4
Tol-Binap, Me (7)	P(Me)(Mes*)	20.0 (1883)	22.5 (2037)	5.9 (1050)	18	128	3
dcpe, CH(Me)(CN) (13)	PHMes*	60.0 (2004)	54.2 (2031)	-81.5 (br)	7	112	
		50 °C	59.8 (1993)	54.4 (2030)	-80.9 (717)	6	112
13a (-60 °C) ^d		61.2 (2043)	54.0 (2035)	-77.7 (720)		119	
13b (-60 °C)		60.9 (2033)	52.6 (2028)	-92.0 (643)		114	
dcpe, CH(Me)(CN) (14)	P(Me)(Ph)	60.0 (1810)	55.6 (2098)	-71 (v br)	8	100	
		90 °C	59.7 ^f (1835)	55.4 (2094)	-74.7 (754)	8	98
14a (22 °C) ^d		59.7 ^f (1835)	55.7 (2082)	-65.7 (814)	8	105	
14b (22 °C)		59.6 (1849)	55.3 (2097)	-77.5 (746)	8	100	
14a (-20 °C)		59.6 (1852)	55.7 (2093)	-66.5 (824)	8	106	

^a Temperature = 22 °C except where noted. Chemical shifts in ppm, external ref 85% H₃PO₄, coupling constants in Hz. P₁ and P₂ are the diphos P nuclei; P₃ is trans to P₁. ^b $n = 0$ for **1**, **5–7**, and **13** and **14**; $n = 1$ for **2–4**. ^c Solvents: toluene-*d*₈ for **1**, **5**, **14**; CD₂Cl₂ for **3**, **4a**, and Pt(Tol-Binap)(Me)(Cl); CDCl₃ for **2**, **4b**; C₆D₆ for **6**, **7**; THF-*d*₆ for **13**. ^d Isomer ratios: 1:1 for **2**, 3:1 for **3**, 7:3 for **13**, 65:35 for **14**. Labels: major isomer a, minor isomer b. ^e The Pt satellites on the Tol-Binap signals were not resolved. ^f P₁ resonance is an average signal for the two isomers.

Scheme 4



2, **5** [Pt] = Pt(Chiraphos), R = Ph, R' = Is

3, **6** [Pt] = Pt(Chiraphos), R = Me, R' = Mes*

4, **7** [Pt] = Pt(R-Tol-Binap), R = Me, R' = Mes*

a few hours causes conversion to a single diastereomer, which can be isolated in pure form. The coordinated secondary phosphines in cations **2–4** show characteristic $J_{\text{Pt-P}}$ (2532–2736 Hz), J_{PP} (375–410 Hz), and J_{PH} (347–384 Hz) coupling constants, as well as weak PH IR stretches at 2400 cm⁻¹ (see Table 1 and the Experimental Section).¹⁰

¹H and ¹³C NMR spectra of the bulky aryl groups in

cations **2–4** provide information about the symmetry and dynamics of these compounds. The chiral centers in **2** cause the *o*-isopropyl methyl groups of the isityl group to be diastereotopic; as expected, they give rise to two different ¹H and ¹³C signals for both **2a** and **2b** in the NMR spectra. In the ¹H NMR spectrum, these protons appear as four doublets at δ 0.97, δ 0.96, δ 0.82, and δ 0.80 (the two upfield signals overlap to give an apparent triplet), all with coupling to the methine proton of approximately 6 Hz. In the ¹³C NMR spectrum, four singlets between δ 24.4 and δ 24.0 are assigned to the isopropyl methyl carbons. Overlapping resonances due to the ortho and para Mes* *t*-Bu groups of **3a** and **3b** appear in the ¹H NMR spectrum at δ 1.39 and δ 1.25, respectively. The ortho signal is broad, presumably due to hindered rotation around the P–C bond of the bulky Mes* group. Similar broadening is observed in the ¹³C NMR peaks due to these *tert*-butyl groups. The ¹H NMR spectrum of **4** shows three *t*-Bu signals, two due to *o*-

(10) Appleton, T. G.; Bennett, M. A. *Inorg. Chem.* **1978**, *17*, 738–747.

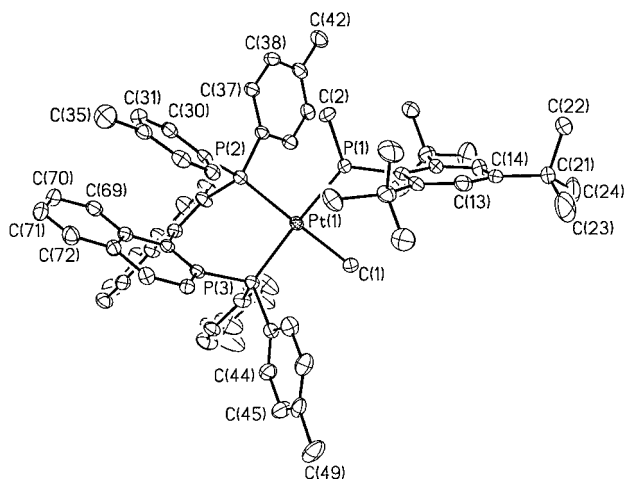


Figure 1. ORTEP diagram of $[\text{Pt}(\text{R-Tol-Binap})(\text{Me})(\text{PH}(\text{Me})\text{Mes}^*)][\text{BF}_4] \cdot 3 \text{CH}_2\text{Cl}_2$ (**4**). Thermal ellipsoids at 30% probability. Counterion, solvent molecules, and hydrogen atoms are omitted for clarity. Selected bond lengths (Å) and angles (deg): Pt–C(1) = 2.130(7), Pt–P(1) = 2.353(2), Pt–P(2) = 2.352(2), Pt–P(3) = 2.308(2), P(1)–C(2) = 1.848(8), P(1)–C(11) = 1.843(7), C(1)–Pt–P(1) = 87.7(2), P(1)–Pt–P(2) = 92.09(6), P(2)–Pt–P(3) = 92.48(6), P(3)–Pt–C(1) = 89.0(2), C(1)–Pt–P(2) = 169.1(2), P(1)–Pt–P(3) = 172.28(7).

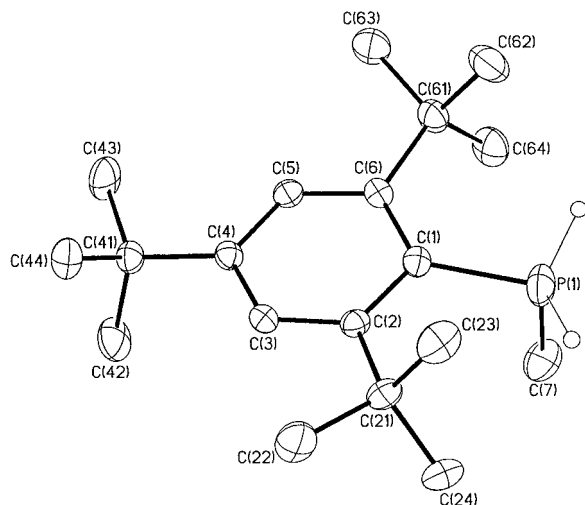


Figure 2. ORTEP diagram of $\text{PH}(\text{Me})(\text{Mes}^*)$ (**8**). Thermal ellipsoids at 30% probability. The two equally occupied positions for the P–H hydrogen are shown; other hydrogen atoms are omitted for clarity. Selected bond lengths (Å) and angles (deg): P(1)–C(7) = 1.829(3), P(1)–C(1) = 1.840(2), P–H (av) = 1.417(6), C(1)–P(1)–C(7) = 99.71(11), H–P–C(1) (av) = 107.65(4), H–P–C(7) (av) = 104.85(4).

t-Bu groups at δ 1.76 and δ 1.49 and one due to a *p*-*t*-Bu group at δ 1.26, indicative of restricted rotation around the P–C(Mes^{*}) bond. Accordingly, four resonances for the two types of carbons on the *o*-*t*-Bu groups are observed in the ¹³C NMR spectrum at 40.5 (*CMe*₃), 39.9 (*CMe*₃), 35.1 (*CMe*₃), and 33.7 (*CMe*₃).

Recrystallization of **4** from CH₂Cl₂/ether produced crystals of a dichloromethane solvate suitable for X-ray crystallography. For comparison, crystals of the secondary phosphine $\text{PH}(\text{Me})(\text{Mes}^*)$ (**8**) were obtained from methanol; the ORTEP diagrams for **4**·3CH₂Cl₂ and **8** are shown in Figures 1 and 2, respectively, with selected bond lengths and angles. The crystallographic data are

given in Table 2, and further details are in the Experimental Section and the Supporting Information.

Two equally occupied positions for the hydrogen atom were located in **8**, and the average P–H distance is 1.417(6) Å, similar to previously reported P–H distances in secondary phosphines, 1.36(7) Å in PHMe_2 ¹¹ and 1.30(1) Å in $\text{PH}(\text{Ph})(\text{Is})$.¹² The C(Mes^{*})–P–C(Me) angle is 99.71(11)°, while the average H–P–C(Me) and H–P–C(Mes^{*}) angles are 104.85(4)° and 107.65(4)°, respectively.

The hydrogen atom on the coordinated phosphine in Pt complex **4** could not be located, but the P–C bond distances do not change significantly on complexation: compare 1.840(2) Å [P–C(Mes^{*})] and 1.829(3) [P–C(Me)] in **8** to the P–C bond distances of 1.843(7) Å [P–C(Mes^{*})] and 1.848(8) Å [P–C(Me)] in **4**. The C(Mes^{*})–P–C(Me) angle opens slightly upon complexation (104.5(3)° from 99.71(11)°), as might be expected on going from three- to four-coordinate phosphorus. The geometry at the Pt center in **4** is close to the expected square plane, the angles between adjacent ligands ranging from 92.48(6)° (Tol-Binap bite angle) to 87.7(2)° [P(coordinated phosphine)–Pt–C(Me)]. The Pt–P(phosphine) bond distance is 2.353(2) Å, which is the same as the Pt–P(Tol-Binap) bond distance of 2.352(2) Å for the P trans to Me. The Pt–P(Tol-Binap) bond length for the P trans to the secondary phosphine is slightly shorter at 2.308(2) Å, consistent with the trans influence expected from the Pt–P coupling constants (¹*J*_{Pt–P} = 2986 Hz (trans to P) and 1832 Hz (trans to Me)).

Treatment of **2–4** with the appropriate base (LiN(SiMe₃)₂ for **2** and **3**, KO*t*-Bu for **4**) generates the phosphido complexes Pt(diphos^{*})(Me)(PRR') (diphos^{*} = *S,S*-Chiraphos; R = Ph, R' = Is, **5**; R = Me, R' = Mes^{*}, **6**; diphos^{*} = R-Tol-Binap, R = Me, R' = Mes^{*}, **7**) (Scheme 4). The *S,S*-Chiraphos complexes **5** and **6** are bright orange, and **7** is dark purple. They were characterized spectroscopically by ¹H, ³¹P, and ¹³C NMR and IR and by elemental analysis and X-ray crystallography (see below) for **5**, but **6** and **7** decompose in the solid state and could not be obtained analytically pure.

In contrast to the cationic precursors, for which diastereomeric mixtures could be observed, the NMR spectra of neutral complexes **5–7** show only one set of signals, which are characteristic of the expected neutral phosphido complexes (Table 1) and similar to those of the previously described compounds Pt(dppe)(Me)-(PRR').⁷

As in cationic precursor **2**, the *o*-isopropyl methyl groups in **5** are diastereotopic, and in the ¹H NMR spectrum, two doublets (²*J*_{HH} = 7 Hz) at δ 1.24 and δ 1.16 are assigned to these sets of protons. In the ¹³C NMR spectrum, four resonances for the carbons of the *o*-CHMe₂ groups are observed; the methine carbon signals appear at δ 33.9 and δ 33.7 and the methyl carbons at δ 26.0 and δ 24.3. Similar results were observed for the related complex Pt(dppe)(COC₃F₇)-(PPhs).⁸ For **6** and **7**, as in the cationic precursors, restricted rotation about the P–C(Mes^{*}) bond is ob-

(11) Bartlett, R. A.; Olmstead, M. M.; Power, P. P.; Sigel, G. A. *Inorg. Chem.* **1987**, *26*, 1941–1946.

(12) Brauer, D. J.; Bitterer, F.; Dörrenbach, F.; Hebler, G.; Stelzer, O.; Krüger, C.; Lutz, F. Z. *Naturforsch.* **1996**, *51b*, 1183–1196.

Table 2. Crystallographic Data for [Pt(R-Tol-Binap)(Me)(PH(Me)Mes*)][BF₄] (**4**)·3CH₂Cl₂, Pt(S,S-Chiraphos)(Me)(PPhIs) (**5**), and PH(Me)(Mes*) (**8**)

	4·3CH ₂ Cl ₂	5	8
formula	C ₇₁ H ₈₂ BCl ₆ F ₄ P ₃ Pt	C ₅₀ H ₅₉ P ₃ Pt	C ₁₉ H ₃₃ P
fw	1522.88	947.97	292.42
space group	P2 ₁ 2 ₁ 2 ₁	P2 ₁ 2 ₁ 2	P2 ₁ /n
a, Å	17.0739(1)	21.0134(5)	9.958(7)
b, Å	19.0657(1)	22.2821(4)	11.630(2)
c, Å	21.6890(3)	9.5472(2)	16.155(4)
β, deg			92.91(4)
V, Å ³	7060.33(11)	4470.22(16)	1868(1)
Z	4	4	4
cryst color, habit	colorless block	yellow block	colorless block
D(calc), g/cm ³	1.433	1.409	1.039
μ(Mo Kα), cm ⁻¹	23.33	32.79	1.39
temp, K	218(2)	198(2)	244(2)
diffractometer	Siemens P4/CCD	Siemens P4/CCD	Siemens P4
radiation		Mo Kα (λ = 0.71073 Å)	
R(F), % ^a	5.01	2.85	4.80
R(wF ²), % ^a	11.52	7.45	10.78

^a Quantity minimized = $R(wF^2) = \sum [w(F_o^2 - F_c^2)^2] / \sum [(wF_o^2)^2]^{1/2}$; $R = \sum \Delta / \sum (F_o)$, $\Delta = |(F_o - F_c)|$.

served by ¹H NMR; the *o*-*t*-Bu methyl signals are observed at δ 1.98 and 1.97 for **6** and δ 2.28 and δ 2.17 for **7**.

Several interpretations of these results are possible. If the phosphido ligands were planar, only one isomer would be expected. However, related complexes (and **5**, see below) contain pyramidal phosphido groups in the solid state, and ³¹P NMR data are consistent with the same structure in solution.⁷ Assuming pyramidal geometry, the phosphido complexes could exist as single diastereomers, or rapid inversion at phosphorus could give time-averaged NMR signals of the expected isomers. A third explanation is that there is an excess of one isomer, and the minor isomer is present in such low concentration that it cannot be detected by NMR spectroscopy. Finally, coincidental overlap of the NMR signals of the two isomers seems unlikely, given the good separations observed for the cationic precursors. Acquisition of the ³¹P NMR spectra at low temperature was inconclusive; the signals of **6** and **7** remain unchanged at a temperature as low as -90 °C. Complex **5** behaved similarly to **1** in that the peaks due to the phosphido ligand and the dppe phosphorus trans to the methyl become broad and disappear into the baseline of the ³¹P NMR spectrum at -60 °C, again presumably due to hindered rotation about the Pt-P(Ph)(Is) bond.

Since solution data gave ambiguous results on inversion rate, we studied the solid-state structure of phosphido complex **5**. Recrystallization from toluene/petroleum ether at -25 °C gave crystals suitable for X-ray diffraction (for details, see Table 2, the Experimental Section, and the Supporting Information). The ORTEP diagram (Figure 3) shows that the particular crystal selected has the S configuration at the pyramidal phosphido ligand. While consistent with the NMR observations of a single set of resonances, this structure is not necessarily representative of the bulk material and does not rule out rapid inversion in solution.

The structure of **5** (for selected bond lengths and angles see the figure caption) is very similar to that of the two previously reported Pt(II) phosphido methyl complexes Pt(dppe)(Me)(PMes₂) and Pt(dppe)(Me)(PHMes*).⁷ The geometry at the metal center is slightly distorted square planar. The largest angle between ligands is 101.78(5)° [P(Chiraphos)-Pt-P(phosphido)]

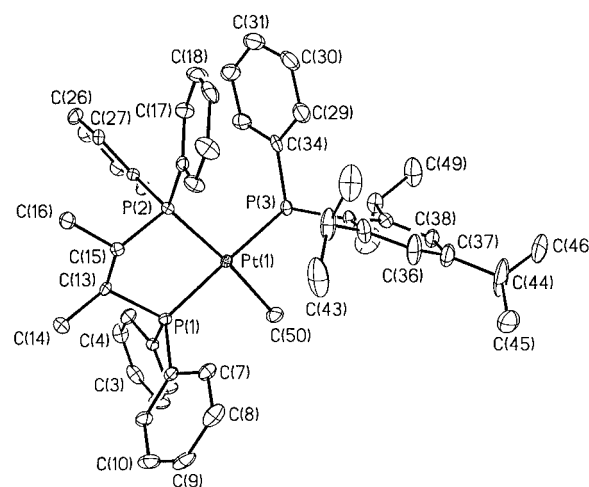


Figure 3. ORTEP diagram of Pt(S,S-Chiraphos)(Me)-(PPhIs) (**5**). Thermal ellipsoids at 30% probability; hydrogen atoms are omitted for clarity. Selected bond lengths (Å) and angles (deg): Pt-C(50) = 2.139(6), Pt-P(3) = 2.3622(15), Pt-P(2) = 2.2972(12), Pt-P(1) = 2.2845(14), C(50)-Pt-P(3) = 84.07(18), P(3)-Pt-P(2) = 101.78(5), P(2)-Pt-P(1) = 85.51(5), P(1)-Pt-C(50) = 89.34(18), C(50)-Pt-P(2) = 173.71(17), P(3)-Pt-P(1) = 164.83(5).

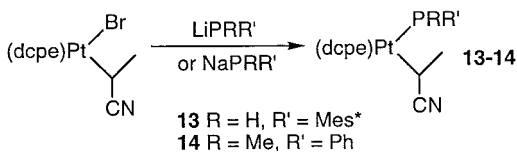
and is presumably due to steric interactions between the Chiraphos phenyl groups and the P(Ph)(Is) ligand. Accordingly, the P(phosphido)-Pt-C(Me) angle (84.07(18) Å) is less than the idealized 90°. The Chiraphos bite angle is 85.51(5)°, and the P(Chiraphos)-Pt-C(Me) angle is 89.34(18)°. The geometry at phosphorus in the P(Ph)(Is) ligand is pyramidal; the sum of the angles at P is 333.3° (compare 328.5° for tetrahedral and 360° for planar geometries). The Pt-P(phosphido) bond length of 2.3622(15) Å is similar to those for the Pt-PMes₂ (2.351(2) Å) and Pt-PHMes* (2.378(5) Å) complexes. The Pt-P(Chiraphos) bond trans to Me is slightly longer than the Pt-P(Chiraphos) bond trans to P(Ph)(Is), 2.2972(12) and 2.2845(14) Å, respectively. This is consistent with a slightly greater trans influence for methyl than for the phosphido ligand and is also reflected in the Pt-P coupling constants from the ³¹P NMR spectrum (1904 and 1981 Hz, respectively).

If the NMR resonances observed for **5**-**7** reflect a single diastereomer in solution, one would expect protonation of the phosphido ligand with HBF₄ to regener-

Table 3. ^{31}P NMR Data for Pt(diphos)(Me)[CH(CN)CH₂PRR'] Complexes^{a-c}

diphos (no.)	PRR'	$\delta(\text{P}_1)$ ($J_{\text{Pt-P}}$)	$\delta(\text{P}_2)$ ($J_{\text{Pt-P}}$)	$\delta(\text{P}_3)$ ($J_{\text{Pt-P}}$)	J_{13}	isomer ratio
dppe (9a) ^d	P(Mes)(Men)	45.3 (2176)	47.8 (1837)	-17.0 (221)	26	2.2
9b		46.0 (2200)	48.6 (1819)	-18.8 (228)	26	2
9c		46.5 (2200)	48.4 (1804)	-15.0 (227)	26	1.1
9d		45.9 (2160)	47.4 (1843)	-10.0 (247)	29	1
Chiraphos (10a-d) ^e	P(Ph)(Is)	58.6-55.9, 51.2-49.9, 48.1-47.1, 43.3-42.6, 39.1-38.0		-26.8 (299) -20.7 (296) -22.4 (264)	35 36 27	3 3 1
Chiraphos (11a-d) ^e	P(Me)(Mes*)	56.2-53.8, 48.8-47.9, 45.8-45.0, 41.1-40.6, 36.5-36.2		-23.4 (235) -19.2 (312) -29.1 (297) -33.5 (253)	26 35 34 29	2 3 12 2
Tol-Binap (12a-d) ^e	P(Me)(Mes*)	34.0-29.6, 24.5-23.7, 22.5-21.2, 20.3-20.0, 17.0-16.1, 10.8-10.2		-36.2 (f) -27.3 (f) -28.3 (260) -32.5 (f) -35.1 (262)	26 42 24 41 26	1 1 3 1 2

^a Temperature = 22 °C. Chemical shifts in ppm, external ref 85% H₃PO₄, coupling constants in Hz. ^b P₁ and P₂ are the diphos P nuclei; the [CH(CN)(CH₂PRR')] group, which contains P₃, is trans to P₁. ^c Solvents: toluene-*d*₈ for **9**, C₆D₆ for **10**, THF for **11**, **12**. ^d For **9a-d**, $J_{12} = 3$ Hz. ^e For **10-12**, the diphos P signals are multiplets for which assignments and identification of Pt-P couplings were not possible. ^f The low concentrations of **11d**, **12a**, and **12c** made it impossible to resolve the Pt-P couplings.

Scheme 6

oxidative addition of CH(Me)(CN)(Br) to Pt(0) and the conversion of Pt(dcppe)[CH(Me)(CN)](Br) (dcpe = Cy₂-PCH₂CH₂PCy₂, Cy = cyclo-C₆H₁₁) to Pt(dcppe)[CH(Me)(CN)](PHMes*) (**13**) by treatment with LiPHMes* (Scheme 6).^{1b} Similarly, reaction of NaP(Me)(Ph) with Pt(dcppe)[CH(Me)(CN)](Br) gives Pt(dcppe)[CH(Me)(CN)](PMePh) (**14**, Scheme 6). The IR spectrum of **14** ($\nu_{\text{CN}} = 2185$ cm⁻¹) is similar to that of **13**.

Since the CH(Me)(CN) ligand is racemic, it is highly unlikely that only one diastereomer of these complexes can be present in solution. This is in contrast to phosphido complexes **1** and **5-7**, which contain homochiral centers, and suggests that NMR observation of the two expected diastereomers should be possible.

At room temperature in THF-*d*₈ solution, the $^{31}\text{P}\{^1\text{H}\}$ NMR spectrum of **13** shows only one set of peaks, including a broad phosphido resonance at $\delta -81.5$ (Table 1). At -60 °C, this signal decoalesces into two separate peaks at $\delta -77.7$ (d, $^2J_{\text{PP}} = 119$, $^1J_{\text{Pt-P}} = 720$ Hz, major) and -92.0 (d, $^2J_{\text{PP}} = 114$, $^1J_{\text{Pt-P}} = 643$ Hz, minor) in a 7:3 ratio. At this temperature the dcpe resonances are also observed for both species. At 50 °C in THF-*d*₈, an average spectrum including a sharper phosphido resonance is observed. Variable-temperature spectra in toluene-*d*₈ (Experimental Section) are similar to those in THF-*d*₈.

Similarly, the room-temperature ^1H NMR spectrum (THF-*d*₈) shows one set of peaks, including a PH signal at $\delta 5.18$ (br dd, 1H, $^2J_{\text{PH}} = 209$, $^3J_{\text{PH}} = 8$, $^2J_{\text{Pt-H}} = 56$ Hz). Rotation about the P-C(Mes*) bond is slow on the NMR time scale, giving rise to two different *o-t*-Bu signals at 1.67 and 1.66 ppm. At -40 °C, signals due to the two different isomers are observed, including PH resonances at $\delta 5.27$ (br d, 1H, $^1J_{\text{PH}} = 210$ Hz, major) and 4.94 (br d, 1H, $^1J_{\text{PH}} = 205$ Hz, minor).

For complex **14**, the two expected diastereomers can be observed by ^{31}P NMR at room temperature in

Table 4. Variable-Temperature NMR Data for Chiral Pt[CH(Me)(CN)] Phosphido Complexes^a

complex	resonance ^b	$\Delta\nu$ (Hz) ^c	T_c (K)	ΔG_c^\ddagger (kcal/mol)
13	<i>PHMes*</i>	2894	273	11.2
	<i>cis dcpe P</i>	268	258	11.7
	<i>trans dcpe P</i>	59	243	11.8
	<i>PHMes*</i>	165	243	11.3
14	<i>PMePh</i>	2214	363	15.3
	<i>cis dcpe P</i>	71	328	16.0
	<i>trans dcpe P</i>	11	298	15.6

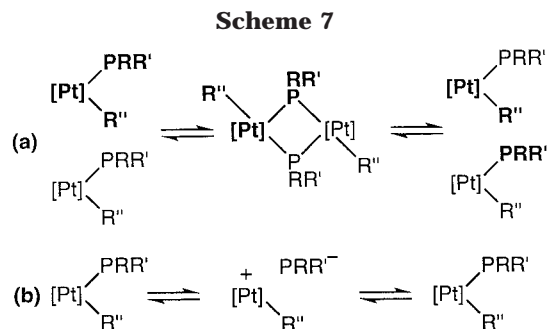
^a Solvent: THF-*d*₈ for **13**, toluene-*d*₈ for **14**. Estimated errors are different for each resonance; "typical" errors are 5 Hz in $\Delta\nu$; 10 °C in T_c , and 0.5 kcal/mol in ΔG_c^\ddagger . Cis and trans are defined with respect to the phosphido ligand. ^b Appropriate nucleus in italics. ^c $\Delta\nu$ values from slow-exchange spectra at -60 °C (^{31}P , **13**), -40 °C (^1H , **13**), and -20 °C (**14**).

toluene-*d*₈ in a 65:35 ratio (Table 1). Peaks due to the dcpe phosphorus cis to the phosphido ligand are resolved for the two isomers and show coupling constants similar to those for **13**. An average signal is observed for the other dcpe P. On heating, the two sets of ^{31}P NMR peaks (phosphido and cis dcpe) resolved at room temperature coalesce, while at low temperature the trans dcpe resonance is resolved as two closely spaced signals.

These data are consistent with fluxional processes involving a combination of phosphorus inversion and rotation about the Pt-P bond, which operate on the NMR time scale for **13** and **14** and thus interconvert the two diastereomers of these complexes. By measuring the coalescence temperatures of the ^{31}P and/or ^1H NMR signals, approximate values for the barriers to these processes were obtained by standard methods.¹⁶ Some details of the NMR studies and the ΔG^\ddagger values obtained (ca. 11.5 kcal/mol for **13** and 15.5 kcal/mol for **14**) are shown in Table 4.

In the literature on metal phosphido complexes, it has been assumed that the fluxional process associated with such barriers is a combination of phosphorus inversion and rotation about the M-P bond. The interconversion of diastereomers might, however, occur by different pathways, two of which are illustrated in Scheme 7. In one, an intermediate with five-coordinate platinum and bridging phosphido groups fragments by Pt-P cleavage

(16) Friebolin, H. *Basic One- and Two-Dimensional NMR Spectroscopy*, 2nd ed.; VCH: Weinheim, 1993.



to exchange phosphido ligands between metal centers, resulting in inversion at phosphorus (Scheme 7a). In the other, reversible ionization of the Pt–P bond to give an ion pair could interconvert the isomers (Scheme 7b). To test these possibilities, we recorded variable-temperature NMR spectra of **13** at concentrations differing by a factor of 3 and in solvents of differing polarity (THF and toluene). As no changes in the temperature dependence of the spectra were seen, it is likely that the possibilities of Scheme 7 are not important in this system and that the measured barriers are indeed those for the P inversion and rotation process.

Conclusions

We prepared platinum(II) phosphido complexes Pt(diphos)(Me)(PRR') containing a fixed chiral center either at a phosphido substituent or at the diphosphine ligand, as well as two Pt(dcpe)[CH(Me)(CN)](PRR') complexes with a chiral Pt alkyl group. For the first two classes of compounds, there is indirect evidence for rapid phosphorus (PRR') inversion on the NMR time scale. The cationic precursors [Pt(diphos*)(Me)(PHRR')]⁺ exist as a mixture of diastereomers, but NMR spectra of the neutral phosphido complexes show only a single set of resonances even at low temperature, and Pt(Chiraphos)(Me)[P(Ph)(Is)] crystallized as a single diastereomer. These observations are consistent with the presence of only one diastereomer in solution, but could also be explained by rapid inversion at the phosphido phosphorus or by the presence of a diastereomeric mixture greatly enriched in one isomer. However, the reactivity of these complexes (protonation and acrylonitrile insertion) is not consistent with the single-diastereomer model and is instead most easily explained by rapid phosphorus inversion. For the CH(Me)(CN) complexes, low-barrier phosphorus inversion processes could be observed directly by variable-temperature NMR spectroscopy, and we have made similar observations in closely related Pt(II) fluoroacyl phosphido complexes.⁸

We have also shown that chiral Pt(II) phosphido complexes undergo diastereoselective acrylonitrile insertion. The origin of the stereoselection and the application of these results to the catalytic asymmetric preparation of tertiary phosphines from racemic secondary phosphines is currently under investigation. In particular, the relative rates of phosphorus inversion and acrylonitrile insertion shown in Scheme 2 will determine if such catalytic reactions are enantioselective.

Experimental Section

General Procedures. Unless otherwise noted, all reactions and manipulations were performed in dry glassware under a

nitrogen atmosphere at 20 °C in a drybox or using standard Schlenk techniques. Petroleum ether (bp 38–53 °C), ether, THF, and toluene were dried and distilled before use from Na/benzophenone. CH₂Cl₂ and acetonitrile were distilled from CaH₂.

Unless otherwise noted, all NMR spectra were recorded on a Varian 300 MHz spectrometer. ¹H and ¹³C NMR chemical shifts are reported relative to Me₄Si and were determined by reference to the residual ¹H or ¹³C solvent peaks. ³¹P NMR chemical shifts are reported relative to H₃PO₄ (85%) used as an external reference. Unless otherwise noted, peaks in NMR spectra are singlets. Coupling constants are reported in hertz (Hz). Infrared spectra were recorded on a Perkin-Elmer 1600 series FTIR machine and are reported in cm⁻¹ for KBr pellets. Elemental analyses were provided by Schwarzkopf Microanalytical Laboratory. Unless otherwise noted, reagents were from commercial suppliers. The following compounds were made by the literature procedures: Pt(dppe)(Me)(OMe),¹⁷ PH(Mes)(Men),^{3a} Pt(COD)(Me)(Cl),¹⁸ Pt(*S,S*-Chiraphos)(Me)(Cl),⁹ PH(Ph)(Is),¹² PH(Me)(Mes*),¹⁹ PH(Me)(Ph).²⁰

Pt(dppe)(Me)[P(Mes)(Men)] (1). Racemic mesityl(–)-(menthyl)phosphine (140 mg, 0.48 mmol) and Pt(dppe)(Me)(OMe) (286 mg, 0.45 mmol) were combined in ca. 4 mL of THF to give an orange solution with a little yellow solid remaining. The solution was filtered through Celite, layered with petroleum ether, and cooled to –20 °C to give, after 1 day, large yellow crystals. The crystals were collected and washed with three 2 mL portions of petroleum ether to give 89 mg of orange solid. The initial petroleum ether washes were yellow, and this complex has some solubility in this solvent, so solvent was evaporated from the combined mother liquor and washes and the residue was recrystallized from ca. 1–2 mL of THF by layering with petroleum ether as above to give, after washing, 104 mg of light orange-yellow crystals, which formed an orange powder on drying (total yield = 193 mg, 49%). A sample for analysis was recrystallized a second time from THF/petroleum ether to give yellow-orange crystals. The reaction was quantitative according to ³¹P NMR, so additional material can be recovered from the filtrate. ¹H NMR (toluene-*d*₆, 21 °C): δ 7.81–7.66 (m, 6H, Ar), 7.45–7.41 (m, 2H, Ar), 7.12–6.98 (m, 12H, Ar), 6.79 (2H, Ar), 3.78–3.65 (m, 1H, CHMe₂), 3.01 (6H, *o*-Me), 2.11 (3H, *p*-Me), 2.28–0.70 (m, 13H, unresolved dppe + menthyl resonances), 1.19 (d, *J* = 7.2, 3H, CHMe₂), 0.88 (m, ²*J*_{Pt–H} = 72, 3H, Pt–Me), 0.76 (d, *J* = 6.6, 3H, CHMe₂), 0.63 (3H, menthyl CHMe). IR: 2917, 1484, 1436, 1186, 1102, 999, 881, 823, 746, 692, 647, 532, 484. Anal. Calcd for C₄₆H₅₇P₃Pt: C, 61.52; H, 6.41. Found: C, 61.25; H, 6.36.

[Pt(*S,S*-Chiraphos)(Me)(PH(Ph)Is)][BF₄] (2). To a stirred solution of Pt(*S,S*-Chiraphos)(Me)(Cl) (205 mg, 0.305 mmol) and PH(Ph)Is (105 mg, 0.336 mmol) in CH₂Cl₂ (7 mL) was added AgBF₄ (59 mg, 0.31 mmol) dissolved in CH₃CN (3 mL). Immediate formation of AgCl was observed, and the reaction mixture was stirred vigorously at room temperature for 30 min. The reaction mixture was filtered and the solvent removed under vacuum. The white residue was washed with three 2 mL portions of ether, dried, and dissolved in a minimum amount of CH₂Cl₂. The CH₂Cl₂ solution was filtered, and ether was added. Cooling of this solution to –25 °C gave 288 mg (91%) of a 1:1 mixture of diastereomers in two crops. A sample for analysis was recrystallized two times from CH₂-Cl₂/ether. The NMR spectra are reported as a mixture of diastereomers (a and b) unless otherwise indicated. ¹H NMR (CDCl₃): δ 7.82–7.56 (m, 15H, Ar), 7.42–7.21 (m, 6H, Ar), 7.12–6.92 (m, 6H, Ar), 7.02 (dd, ¹*J*_{PH} = 384, ³*J*_{PH} = 6, 1H, PH-

(17) Bryndza, H. E.; Calabrese, J. C.; Wreford, S. S. *Organometallics* **1984**, *3*, 1603–1604.

(18) Clark, H. C.; Manzer, L. E. *J. Organomet. Chem.* **1973**, *59*, 411–428.

(19) See ref 12 and ref 5b therein.

(20) Roberts, N. K.; Wild, S. B. *J. Am. Chem. Soc.* **1979**, *101*, 6254–6260.

(Ph)Is, diastereomer b), 6.45 (dd, $^1J_{\text{PH}} = 375$, $^3J_{\text{PH}} = 10$, 1H, PH(Ph)Is, diastereomer a), 3.10–2.99 (m, 2H, *o*-CHMe₂), 2.92–2.83 (m, 1H, *p*-CHMe₂), 2.51–2.23 (m, 2H, CHMe), 1.25–1.21 (m, 6H, *p*-CHMe₂), 1.18–1.01 (m, 6H, CHMe), 0.97 (d, $^3J_{\text{HH}} = 6$, 3H, *o*-CHMe₂), 0.96 (d, $^3J_{\text{HH}} = 6$, 3H, *o*-CHMe₂), 0.82 (d, $^3J_{\text{HH}} = 6$, 3H, *o*-CHMe₂), 0.80 (d, $^3J_{\text{HH}} = 6$, 3H, *o*-CHMe₂), 0.39–0.32 (m, $^2J_{\text{Pt-H}} = 60$, 3H, Pt–Me). $^{13}\text{C}\{^1\text{H}\}$ NMR (CDCl₃): δ 153.0–152.7 (m, quat. Ar), 136.0–135.5 (m, Ar), 134.2–134.1 (m, Ar), 132.9 (broad, Ar), 132.4–132.0 (m, Ar), 131.2–130.8 (m, Ar), 129.6–128.9 (m, Ar), 128.6–128.4 (m, Ar), 127.0–123.3 (m, quat. Ar), 122.8–122.5 (m, Ar), 38.5–36.0 (m, CHMe), 34.1 (*p*-CHMe₂, b), 34.0 (*p*-CHMe₂, a), 33.2 (d, $^3J_{\text{PC}} = 10$, *o*-CHMe₂, a), 33.0 (d, $^3J_{\text{PC}} = 10$, *o*-CHMe₂, b), 24.4 (*o*-CHMe₂, a), 24.2 (*o*-CHMe₂, a), 24.1 (*o*-CHMe₂, b), 24.0 (*o*-CHMe₂, b), 23.6 (*p*-CHMe₂, a), 23.5 (*p*-CHMe₂, b), 14.0–13.2 (m, CHMe), 2.2 (dm, $^2J_{\text{PC}} = 70$, Pt–Me, b, Pt satellites were not resolved), 0.2 (dm, $^2J_{\text{PC}} = 65$, Pt–Me, a, Pt satellites were not resolved). IR: 3055, 2955, 2877, 2400 (w, PH), 1533, 1477, 1438, 1400, 1366, 1311, 1277, 1233, 1211, 1183, 1055 (BF₄), 916, 883, 750, 688, 550, 527. Anal. Calcd for C₅₀H₆₀BF₄P₃Tp: C, 57.97; H, 5.85. Found: C, 57.52; H, 5.83.

[Pt(S,S-Chiraphos)(Me)(PH(Me)Mes*)][BF₄] (3). To a stirred slurry of Pt(S,S-Chiraphos)(Me)(Cl) (320 mg, 0.476 mmol) in CH₂Cl₂ (10 mL) was added a solution of AgBF₄ (93 mg, 0.48 mmol) dissolved in CH₃CN (2 mL). Immediate reaction occurred as indicated by the formation of AgCl. PH(Me)(Mes*) (153 mg, 0.524 mmol) dissolved in CH₂Cl₂ (2 mL) was added to the reaction mixture, which was stirred vigorously for 30 min. The pale yellow solution was filtered, and the solvent was removed under vacuum. The white solid was washed with ether (three 5 mL portions) and dried. Recrystallization from CH₂Cl₂/ether at –25 °C yielded 387 mg (80%) of a mixture of diastereomers in a ratio of approximately 3:1. The NMR spectra are reported as a mixture of diastereomers (a and b) unless otherwise indicated. ^1H NMR (CD₂Cl₂): δ 8.02–7.45 (broad m, 22H, Ar), 6.80 (dm, $^1J_{\text{PH}} = 383$, 1H, PH, diastereomer b), 6.03 (dm, $^1J_{\text{PH}} = 374$, 1H, PH, diastereomer a), 2.29–2.16 (m, 2H, CHMe), 1.39 (broad, 21H, *o*-CMe₃ and PMe), 1.25 (broad, 9H, *p*-CMe₃), 1.13–1.07 (broad m, 6H, CHMe), 0.44 (m, $^2J_{\text{Pt-H}} = 60$, Pt–Me, a), 0.04 (m, $^2J_{\text{Pt-H}} = 60$, Pt–Me, b). $^{13}\text{C}\{^1\text{H}\}$ NMR (CD₂Cl₂): δ 155.8–155.6 (m, quat. Ar), 155.5–154.7 (broad m, quat. Ar), 152.7 (quat. Ar), 152.5 (quat. Ar), 136.9–136.4 (m, Ar), 133.8 (Ar), 133.4–133.2 (m, Ar), 133.2 (Ar), 132.7–131.5 (m, Ar), 130.1–129.2 (m, Ar), 128.3–123.2 (m, quat. Ar), 118.6 (quat. Ar), 118.0 (quat. Ar), 39.9–39.3 (m, CHMe), 39.2 (*o*-CMe₃), 38.8–38.4 (broad, *o*-CMe₃), 37.9–36.5 (m, CHMe), 35.1 (*p*-CMe₃), 34.2 (*o*-CMe₃), 34.2–33.8 (broad, *o*-CMe₃), 30.9 (*p*-CMe₃), 14.8 (dm, $^1J_{\text{PC}} = 36$, P–Me), 14.1–13.4 (m, CHMe), 7.2 (dm, $^2J_{\text{PC}} = 72$, $^1J_{\text{Pt-C}} = 528$, Pt–Me, a), 3.2 (dm, $^1J_{\text{PC}} = 71$, Pt–Me, b, Pt satellites were not resolved). IR: 2955, 2877, 2400 (w, PH), 1538, 1477, 1433, 1361, 1183, 1061 (BF₄), 916, 883, 750, 694, 550, 527. Anal. Calcd for C₄₈H₆₄BF₄P₃Pt: C, 56.74; H, 6.36. Found: C, 56.26; H, 6.00.

Pt(R-Tol-Binap)(Me)(Cl). In the air, to a stirred solution of Pt(COD)(Me)(Cl) (350 mg, 0.98 mmol) dissolved in CH₂Cl₂ (5 mL) was added R-Tol-Binap (671 mg, 0.98 mmol) dissolved in CH₂Cl₂ (2 mL). The pale yellow solution was stirred at room temperature for 10 min. The solvent was removed in vacuo, and the resulting solid was washed with three 2 mL portions of ether. The solid was recrystallized from CH₂Cl₂/ether at –25 °C to yield 703 mg (77%) of pale yellow Pt(R-Tol-Binap)(Me)(Cl). ^1H NMR (CD₂Cl₂): δ 7.73–7.28 (broad m, 20H, Ar), 7.06–7.03 (m, 2H, Ar), 6.70–6.62 (m, 2H, Ar), 6.48–6.42 (m, 4H, Ar), 2.45 (6H, *p*-tol Me), 1.99 (3H, *p*-tol Me), 1.98 (3H, *p*-tol Me), 0.44 (dd, $^3J_{\text{PH}} = 8$, $^2J_{\text{Pt-H}} = 55$, 3H, Pt–Me). $^{13}\text{C}\{^1\text{H}\}$ NMR (CD₂Cl₂): δ 141.1 (Ar), 140.6 (Ar), 140.4 (Ar), 139.9 (Ar), 139.4–139.3 (m, Ar), 137.6–137.4 (m, Ar), 136.1–135.9 (m, Ar), 135.2–134.8 (m, Ar), 134.0 (Ar), 133.7 (Ar), 133.6 (Ar), 133.2 (Ar), 133.1 (m, Ar), 132.5 (Ar), 132.0 (Ar), 131.2 (Ar), 130.4 (Ar), 128.8–127.8 (m, Ar), 127.6 (Ar), 127.4 (Ar), 127.2

(Ar), 127.0 (Ar), 126.7 (Ar), 126.4 (Ar), 126.3 (Ar), 126.2 (Ar), 126.0 (Ar), 125.0 (Ar), 123.7 (Ar), 123.2 (Ar), 122.1 (Ar), 121.3 (Ar), 21.5 (*p*-tol Me), 21.4 (*p*-tol Me), 21.2 (*p*-tol Me), 21.1 (*p*-tol Me), 11.2 (dd, $^2J_{\text{PC}} = 97$, 6, Pt–Me, Pt satellites were not resolved). Anal. Calcd for C₄₉H₄₃ClP₂Pt·2/3Et₂O: C, 63.73; H, 5.14. Found: C, 63.40; H, 5.17. The presence of ether in the analytical sample was confirmed by ^1H NMR.

[Pt(R-Tol-Binap)(Me)(PH(Me)Mes*)][BF₄] (4). To a stirred solution of Pt(R-Tol-Binap)(Me)(Cl) (302 mg, 0.33 mmol) in CH₂Cl₂ (5 mL) was added AgBF₄ (64 mg, 0.33 mmol) dissolved in CH₃CN (5 mL). Immediate formation of AgCl occurred, as indicated by a white precipitate. PH(Me)Mes* (105 mg, 0.36 mol) dissolved in CH₂Cl₂ (2 mL) was added to the reaction mixture, which was stirred vigorously for 2 h. The pale yellow solution was filtered, and the solvent was removed in vacuo. The resulting solid was washed with three 2 mL portions of petroleum ether. Recrystallization from CH₂Cl₂/ether at –25 °C yielded 329 mg (80%) of a pale yellow crystalline solid shown to be a single diastereomer by NMR. ^1H NMR (CD₂Cl₂): 7.71–7.29 (m, 18H, Ar), 7.09–7.01 (m, 6H, Ar), 6.50–6.39 (m, 6H, Ar), 6.17 (dm, $^1J_{\text{PH}} = 381$, 1H, PH), 2.51 (3H, *p*-tol Me), 2.42 (3H, *p*-tol Me), 2.01 (6H, *p*-tol Me), 1.76 (9H, *o*-CMe₃), 1.49 (9H, *o*-CMe₃), 1.26 (9H, *p*-CMe₃), 1.04–0.98 (m, $^3J_{\text{Pt-H}} = 24$, 3H, PMe), 0.13–0.06 (m, $^2J_{\text{Pt-H}} = 59$, 3H, Pt–Me). $^{13}\text{C}\{^1\text{H}\}$ NMR (CD₂Cl₂): δ 154.6 (Ar), 154.5 (Ar), 153.6 (Ar), 152.6–152.5 (m, Ar), 143.0 (Ar), 142.2 (Ar), 141.9 (Ar), 141.7 (Ar), 135.5–135.2 (m, Ar), 134.9–134.6 (m, Ar), 134.3 (Ar), 134.1 (Ar), 133.6 (Ar), 130.3 (Ar), 130.2 (Ar), 129.1–128.9 (m, Ar), 128.4–127.8 (m, Ar), 126.9 (Ar), 126.8 (Ar), 123.5 (Ar), 121.5 (Ar), 120.8 (Ar), 40.5 (*o*-CMe₃), 39.9 (*o*-CMe₃), 35.2 (*p*-CMe₃), 35.1 (*o*-CMe₃), 33.7 (*o*-CMe₃), 30.9 (*p*-CMe₃), 21.5 (*p*-tol Me), 21.4 (*p*-tol Me), 21.3 (*p*-tol Me), 21.2 (*p*-tol Me), 14.3 (d, $^1J_{\text{PC}} = 36$, PMe), 9.5 (d, $^2J_{\text{PC}} = 68$, Pt–Me, Pt satellites were not resolved). IR: 2955, 2866, 2400 (w, PH), 1555, 1494, 1450, 1400, 1361, 1305, 1222, 1188, 1055 (BF₄), 916, 872, 805, 744, 694, 672, 650, 600, 511, 433. Anal. Calcd for C₆₈H₇₆BF₄P₃Pt: C, 64.40; H, 6.05. Found: C, 64.04; H, 6.17.

Pt(S,S-Chiraphos)(Me)[P(Ph)Is] (5). To a stirred slurry of [Pt(S,S-Chiraphos)(Me)(PH(Ph)Is)][BF₄] (396 mg, 0.382 mmol) in THF (5 mL) was added LiN(SiMe₃)₂ (121 mg, 0.722 mmol) dissolved in THF (5 mL). The reaction mixture immediately became homogeneous and bright orange and was stirred at room temperature for 1 h. The solvent was removed under vacuum, and the orange solid was washed twice with petroleum ether (5 mL) and dried. The solid was extracted with toluene (20 mL) and filtered. The filtrate was concentrated under vacuum (to approximately 5 mL). Petroleum ether was added to the toluene solution, and cooling of this solution to –25 °C gave 284 mg (78%) of orange solid in two crops. ^1H NMR (toluene-*d*₆): δ 7.92–7.79 (m, 4H, Ar), 7.54–7.48 (m, 2H, Ar), 7.15–6.98 (m, 18H, Ar), 6.69–6.58 (m, 3H, Ar), 4.70–4.55 (m, 2H, *o*-CHMe₂), 2.98 (septet, $^3J_{\text{HH}} = 7$, 1H, *p*-CHMe₂), 1.94 (broad, 2H, CHMe), 1.25 (d, $^3J_{\text{HH}} = 7$, 6H, *p*-CHMe₂), 1.24 (d, $^3J_{\text{HH}} = 7$, 6H, *o*-CHMe₂), 1.16 (d, $^3J_{\text{HH}} = 7$, 6H, *o*-CHMe₂), 0.69–0.63 (m, 3H, CHMe), 0.67–0.63 (m, 3H, $^2J_{\text{Pt-H}} = 67$, Pt–Me), 0.58–0.52 (m, 3H, CHMe). $^{13}\text{C}\{^1\text{H}\}$ NMR (toluene-*d*₆): δ 155.2–155.1 (m, quat. Ar), 147.6 (quat. Ar), 137.1–136.6 (m, Ar), 133.7–133.5 (m, Ar), 132.4–132.3 (m, Ar), 132.1–132.0 (m, Ar), 131.2 (Ar), 130.8 (Ar), 130.0 (Ar), 129.4 (Ar), 128.7–127.8 (m, Ar), 126.5–126.4 (m, Ar), 125.4–124.7 (m, quat. Ar), 123.2 (Ar), 121.2–121.1 (m, Ar), 39.3–38.5 (m, CHMe), 36.6–35.8 (m, CHMe), 34.7 (*p*-CHMe₂), 33.9 (*o*-CHMe₂), 33.7 (*o*-CHMe₂), 26.0 (*o*-CHMe₂), 25.2 (*p*-CHMe₂), 24.3 (*o*-CHMe₂), 14.3–14.0 (m, CHMe), 3.1 (d, $^2J_{\text{PC}} = 73$, Pt–Me, Pt satellites were not resolved). IR: 3055, 2955, 2866, 1477, 1433, 1377, 1311, 1277, 1183, 1100, 1055, 933, 877, 744, 694, 527. Anal. Calcd for C₅₀H₅₉P₃Pt: C, 63.34; H, 6.29. Found: C, 62.51; H, 6.28.

Pt(S,S-Chiraphos)(Me)[P(Me)Mes*] (6). To a solution of [Pt(S,S-Chiraphos)(Me)(PH(Me)Mes*)][BF₄] (165 mg, 0.163 mmol) in THF (5 mL) was added a solution of LiN(SiMe₃)₂ (33

mg, 0.20 mmol) in THF (1 mL). The solution immediately turned bright orange. The solvent was removed under vacuum, and the orange residue was extracted with toluene (15 mL) and filtered. The toluene was removed under vacuum and the bright orange-yellow solid was dissolved in warm petroleum ether, filtered, and concentrated to approximately 5 mL. Cooling of this solution to $-25\text{ }^{\circ}\text{C}$ overnight gave 104 mg (69%) of an orange-yellow solid. The compound was stable in solution, but decomposition to an unidentified white solid occurred in the solid state. ^1H NMR (C_6D_6): δ 8.23–8.18 (m, 2H, Ar), 7.99–7.83 (m, 4H, Ar), 7.68–7.65 (m, 2H, Ar), 7.39–7.33 (m, 2H, Ar), 7.25–6.97 (m, 12H, Ar), 1.98 (9H, *o*- CMe_3), 1.97 (9H, *o*- CMe_3), 1.89–1.81 (m, 2H, *CHMe*), 1.81–1.76 (m, 3H, $^3J_{\text{Pt-H}} = 47$, *PMe*), 1.32 (9H, *p*- CMe_3), 0.72–0.59 (m, 6H (*CHMe*) + 3H ($^2J_{\text{Pt-H}} = 69$, Pt–Me)). $^{13}\text{C}\{^1\text{H}\}$ NMR (C_6D_6): δ 158.5–158.4 (m, quat. Ar), 157.8–157.1 (m, quat. Ar), 147.5 (quat. Ar), 142.5–141.9 (m, quat. Ar), 137.6–137.3 (m, Ar), 134.0–133.8 (m, Ar), 132.8–132.6 (m, Ar), 131.8–131.5 (m, Ar), 131.4–131.2 (m, quat. Ar), 130.8 (quat. Ar), 130.2–130.0 (m, Ar), 129.6 (Ar), 129.2 (Ar), 129.1 (Ar), 123.8–123.6 (m, quat. Ar), 123.0–122.8 (m, Ar), 42.6–41.8 (m, *CHMe*), 40.7–40.6 (m, 2 *o*- CMe_3 and *p*- CMe_3), 38.2–37.6 (m, *CHMe*), 35.3–35.1 (m, 2 *o*- CMe_3), 32.0 (*p*- CMe_3), 19.9 (dd, $^1J_{\text{PC}} = 31$, $^3J_{\text{PC}} = 6$, Pt–Me), 15.3–14.8 (m, *CHMe*), 2.0 (ddd, $^2J_{\text{PC}} = 81$, 8, 3, $^1J_{\text{Pt-C}} = 596$, Pt–Me).

Pt(R-Tol-Binap)(Me)(P(Me)Mes*) (7). To a white slurry of [Pt(R-Tol-Binap)(Me)(PH(Me)Mes*)][BF₄] (411 mg, 0.324 mmol) in THF (15 mL) was added potassium *tert*-butoxide (55 mg, 0.49 mmol) dissolved in THF (5 mL). The reaction mixture immediately became dark brownish-red, and the solvent was removed in vacuo. The dark purple solid was dissolved in toluene and filtered. The toluene was removed in vacuo and the residue washed with a minimum amount of cold petroleum ether to give 310 mg (81%) of product. A sample which was pure by ^1H NMR could be recrystallized from petroleum ether at $-25\text{ }^{\circ}\text{C}$. However in the solid state the product decomposed to an unidentified gray solid. ^1H NMR (C_6D_6): δ 8.29–7.67 (m, 8H, Ar), 7.31–7.11 (m, 12H, Ar), 6.98–6.88 (m, 3H, Ar), 6.63–6.54 (m, 5H, Ar), 6.11–6.09 (m, 2H, Ar), 2.28 (9H, *o*- CMe_3), 2.17 (9H, *o*- CMe_3), 2.15 (3H, *p*-tol Me), 2.02 (3H, *p*-tol Me), 1.79 (3H, *p*-tol Me), 1.69 (3H, *p*-tol Me), 1.51–1.46 (m, $^3J_{\text{Pt-H}} = 49$, 3H, *PMe*), 1.33 (9H, *p*- CMe_3), 0.64–0.56 (m, $^2J_{\text{Pt-H}} = 67$, 3H, Pt–Me). $^{13}\text{C}\{^1\text{H}\}$ NMR (C_6D_6): δ 157.9–157.5 (m, quat. Ar), 155.0 (quat. Ar), 147.4 (quat. Ar), 142.1 (quat. Ar), 141.4–141.3 (m, quat. Ar), 140.7 (quat. Ar), 140.3 (quat. Ar), 139.8–139.6 (m, quat. Ar), 139.4–139.2 (m, quat. Ar), 138.2–138.0 (m, quat. Ar), 136.7–135.6 (m, Ar), 134.9–134.8 (m, Ar), 134.3–133.8 (m, quat. Ar), 129.6 (Ar), 128.9–128.1 (m, Ar), 126.6–125.6 (m, Ar), 125.0–124.9 (m, Ar), 124.5–124.4 (m, Ar), 124.0–123.9 (m, Ar), 121.6–121.5 (m, Ar), 41.0 (d, $^3J_{\text{PC}} = 7$, *o*- CMe_3), 40.8 (*o*- CMe_3), 36.2 (broad, *o*- CMe_3), 35.2 (*p*- CMe_3), 34.8 (d, $^4J_{\text{PC}} = 17$, *o*- CMe_3), 31.9 (*p*- CMe_3), 21.8 (*p*-tol Me), 21.7 (*p*-tol Me), 21.5 (*p*-tol Me), 21.4 (*p*-tol Me), 18.5 (dm, $^1J_{\text{PC}} = 39$, *PMe*), 8.9 (ddd, $^2J_{\text{PC}} = 80$, 8, 2, Pt–Me, Pt satellites were not resolved). Anal. Calcd for $\text{C}_{68}\text{H}_{75}\text{P}_3\text{Pt}$: C, 69.18; H, 6.42. Found: C, 71.48; H, 6.73.

Treatment of Pt(S,S-Chiraphos)(Me)[P(Me)Mes*] (6) with HBF₄. To an orange solution of Pt(S,S-Chiraphos)(Me)[P(Me)Mes*] (33 mg, 0.036 mmol) in diethyl ether (2 mL) was added HBF₄·Me₂O (6 μL , 0.04 mmol) via microliter syringe. The orange color quickly faded, and a white precipitate formed. The solvent was pipetted off, and the white solid was dried to give 33 mg (92%) of **3** as a 2:1 mixture of diastereomers, confirmed by ^{31}P and ^1H NMR.

Treatment of Pt(R-Tol-Binap)(Me)[P(Me)Mes*] (7) with HBF₄. To a purple solution of Pt(R-Tol-Binap)(Me)[P(Me)Mes*] (48 mg, 0.041 mmol) in diethyl ether (2 mL) was added HBF₄·Me₂O (7 μL , 0.05 mmol) via microliter syringe. The purple color quickly faded, and an off-white precipitate formed. The solvent was removed under vacuum, and the residue was washed with diethyl ether (2 mL) and dried to give 42 mg (81%) of **4**. ^{31}P

and ^1H NMR showed a mixture of diastereomers of **4** in a ratio of approximately 3:1. Some characteristic resonances of the minor diastereomer could be assigned. ^1H NMR (CDCl_3): δ 0.39 (m, $^1J_{\text{Pt-H}} = 59$, Pt–Me); see Table 1 for ^{31}P NMR data. The ratio of diastereomers does not change over a period of 2 weeks in CDCl_3 or CD_2Cl_2 . However, a sample of the 3:1 mixture of diastereomers in CD_2Cl_2 and one drop of CD_3CN isomerizes to the major diastereomer in 1 day at room temperature. Alternatively, to a solution of the 3:1 diastereomeric mixture (39 mg, 0.031 mmol) in CD_2Cl_2 was added PH-(Me)(Mes*) (3 mg, 0.01 mmol) and one drop of CD_3CN . After 30 min the ^1H and ^{31}P NMR spectra showed complete isomerization to the major diastereomer.

Pt(dppe)(Me)[CH(CN)CH₂P(Mes)(Men)] (9). An excess of acrylonitrile (ca. 0.1 mL) was added via syringe to an NMR tube containing 70 mg of **1** (0.078 mmol) in ca. 1 mL of toluene-*d*₆. The yellow-orange color of **1** bleached quickly, giving a colorless solution within minutes. The $^{31}\text{P}\{^1\text{H}\}$ NMR spectrum showed quantitative conversion to **9** as a mixture of four diastereomers **a–d**. The solvent was removed under vacuum, and the light yellow residue was stirred with petroleum ether (4 \times 3 mL) to give a white powder, sparingly soluble in petroleum ether. The solvent was decanted and the powder dried in vacuo to give 50 mg (67%) of the analytically pure product, which can be further recrystallized from THF/petroleum ether.

Due to the complexity of the ^1H NMR spectrum, complete assignment and integration of the resonances was not possible. ^1H NMR (C_6D_6): δ 7.81–7.41 (m, 7H, Ar), 7.23–6.96 (m, 13H, Ar), 6.76–6.70 (m, 2H, Mes), 3.34–3.29 (m), 2.68 and 2.62 (6H, *o*-Me), 2.14, 2.09, and 2.06 (3H, *p*-Me), 2.80–1.40 (m), 1.33–1.13 (m), 1.05–1.03 (m), 0.98–0.86 (m), 0.70–0.66 (m), 0.43–0.41 (m), 0.38–0.35 (m). IR (KBr): 2949, 2923, 2183, 1435, 1103, 746, 693, 532. Anal. Calcd for $\text{C}_{46}\text{H}_{60}\text{NP}_3\text{Pt}$: C, 61.87; H, 6.37; N, 1.47. Found: C, 61.79; H, 6.81; N, 1.39.

Treatment of Pt(S,S-Chiraphos)(Me)[P(Ph)Is] (5), Pt-(S,S-Chiraphos)(Me)[P(Me)Mes*] (6), and Pt(R-Tol-Binap)(Me)[P(Me)Mes*] (7) with Acrylonitrile. (1) To an NMR tube containing Pt(S,S-Chiraphos)(Me)[P(Ph)Is] (20 mg, 0.022 mmol) in C_6D_6 was added acrylonitrile (30 μL , 0.46 mmol) via microliter syringe. The bright orange color faded to pale yellow immediately. (2) To an NMR tube containing Pt-(S,S-Chiraphos)(Me)[P(Me)Mes*] (50 mg, 0.054 mmol) in THF was added acrylonitrile (5 μL , 0.076 mmol) via microliter syringe. After 30 min, the bright orange color of the solution faded to pale yellow. (3) To an NMR tube containing Pt(R-Tol-Binap)(Me)[P(Me)Mes*] (20 mg, 0.017 mmol) in THF was added acrylonitrile (20 μL , 0.30 mmol) via microliter syringe. After 24 h the color faded to pale yellow. For ^{31}P NMR data, see Table 3.

Crystallographic Structural Determination. Crystal data collection and refinement parameters are given in Table 2. Suitable crystals for single-crystal X-ray diffraction were selected and mounted either in a nitrogen-flushed, thin-walled capillary, and flame sealed, or on the tip of a fine glass fiber with epoxy cement. The data for **4** and **5** were collected on a Siemens P4 diffractometer equipped with a SMART/CCD detector.

The systematic absences in the diffraction data are uniquely consistent with the reported space groups. The structures were solved by direct methods, completed by subsequent difference Fourier syntheses, and refined by full-matrix least-squares procedures. An empirical absorption correction was applied to the data of **4** and **5**, based on a Fourier series in the polar angles of the incident and diffracted beam paths, and was used to model an absorption surface for the difference between the observed and calculated structure factors.²¹ No absorption corrections for **8** were required because there was less than 10% variation in the integrated ψ -scan intensities. Axial

photographs of **5** confirm that no doubling along the *c*-axis was missed and there is no 2_1 screw axis along *c*. Three molecules of dichloromethane were located in the asymmetric unit of **4**, the C–Cl distances were fixed to an average C–Cl distance, and the atoms were refined isotropically. Two equally occupied positions for the hydrogen atom on phosphorus in **8** were located from the difference map and allowed to refine. The hydrogen atom on the phosphorus atom of **4** could not be located from the difference map and was ignored. All other non-hydrogen atoms were refined with anisotropic displacement parameters. All other hydrogen atoms were treated as idealized contributions.

All software and sources of the scattering factors are contained in the SHELXTL (5.03 and 5.10) program libraries (G. Sheldrick, Siemens XRD, Madison, WI).

Pt(dcpce)[CH(Me)(CN)](PHMes*) (13). The synthesis and some characterizing data for this complex were reported previously.^{1b} Additional variable-temperature NMR data (acquired on a 500 MHz instrument) are as follows.

¹H NMR (THF-*d*₈, 22 °C): δ 7.35 (1H, Ar), 7.25 (1H, Ar), 5.18 (br dd, 1H, ²*J*_{PH} = 209, ³*J*_{PH} = 8, ²*J*_{Pt–H} = 56, PH), 2.67 (br m, 1H, CH), 2.50–1.00 (br m, 48H, dcpce), 1.67 (9H, *o*-*t*-Bu), 1.66 (9H, *o*-*t*-Bu), 1.31 (9H, *p*-*t*-Bu), 0.80 (virtual t, 3H, ³*J*_{HH} = 7, ⁴*J*_{PH} = 7, ³*J*_{Pt–H} = 50, Me). ¹H NMR (THF-*d*₈, 50 °C): δ 7.35 (1H, Ar), 7.25 (1H, Ar), 5.18 (ddd, 1H, ²*J*_{PH} = 209, ³*J*_{PH} = 8, ³*J*_{PH} = 2, ²*J*_{Pt–H} = 56, PH), 2.67 (br m, 1H, CH), 2.50–1.00 (br m, 48H, dcpce), 1.67 (9H, *o*-*t*-Bu), 1.66 (9H, *o*-*t*-Bu), 1.31 (9H, *p*-*t*-Bu), 0.80 (virtual t, 3H, ³*J*_{HH} = 7, ⁴*J*_{PH} = 7, ³*J*_{Pt–H} = 50, Me). ¹H NMR (THF-*d*₈, –40 °C): δ 7.34 (1H, Ar, major isomer a), 7.33 (1H, Ar, minor isomer b), 7.24 (1H, Ar, a), 7.23 (1H, Ar, b), 5.27 (br d, 1H, ²*J*_{PH} = 210, PH, a), 4.94 (br d, 1H, ²*J*_{PH} = 205, PH, b), 2.62 (br m, 1H of a + 1H of b, CH), 2.50–1.00 (br m, 48H of a + 48H of b, dcpce), 1.73, 1.68, 1.62 (all s, 18H of a + 18H of b, *o*-*t*-Bu), 1.31 (9H of a + 9H of b, *p*-*t*-Bu), 0.89 (apparent t, 3H of a + 3H of b, ³*J*_{HH} = 7, ⁴*J*_{PH} = 7, ³*J*_{Pt–H} = 50, Me).

³¹P{¹H} NMR (toluene-*d*₈, 22 °C): δ 60.1 (d, ²*J*_{PP} = 103, ¹*J*_{Pt–P} = 1977), 54.4 (¹*J*_{Pt–P} = 2023), –80.5 (br). ³¹P{¹H} NMR (toluene-*d*₈, 90 °C): δ 59.8 (dd, ²*J*_{PP} = 107, 6, ¹*J*_{Pt–P} = 1951), 54.9 (br, ¹*J*_{Pt–P} = 2015), –79.3 (br d, ²*J*_{PP} = 108, ¹*J*_{Pt–P} = 686). ³¹P{¹H} NMR (toluene-*d*₈, –60 °C, major isomer a, ca. 70%): δ 61.1 (d, ²*J*_{PP} = 116, ¹*J*_{Pt–P} = 2041), 53.9 (¹*J*_{Pt–P} = 2016), –76.3 (d, ²*J*_{PP} = 116, ¹*J*_{Pt–P} = 718). ³¹P{¹H} NMR (toluene-*d*₈, –60 °C, minor isomer b, ca. 30%): δ 60.5 (d, ²*J*_{PP} = 109, ¹*J*_{Pt–P} not resolved), 52.4 (¹*J*_{Pt–P} = 2019), –90.7 (d, ²*J*_{PP} = 109, ¹*J*_{Pt–P} = 643). ¹H NMR (toluene-*d*₈, 22 °C): δ 7.62 (1H, Ar), 7.50 (1H, Ar), 5.46 (br dd, 1H, ²*J*_{PH} = 208, ³*J*_{PH} = 8, ²*J*_{Pt–H} = 56, PH), 2.85 (br m, 1H, CH), 2.50–1.00 (br m, 48H of dcpce + 3H of CH(*Me*)CN), 1.94 (9H, *o*-*t*-Bu), 1.87 (9H, *o*-*t*-Bu), 1.42 (9H, *p*-*t*-Bu). ¹H NMR (toluene-*d*₈, 90 °C): δ 7.59 (1H, Ar), 7.47 (1H, Ar), 5.44 (br dd, 1H, ²*J*_{PH} = 208, ³*J*_{PH} = 8, ²*J*_{Pt–H} = 56, PH), 2.85 (br m, 1H, CH), 2.50–1.00 (br m, 48H of dcpce + 3H of CH(*Me*)CN), 1.91 (9H, *o*-*t*-Bu), 1.85 (9H, *o*-*t*-Bu), 1.42 (9H, *p*-*t*-

Bu). ¹H NMR (toluene-*d*₈, –40 °C): 7.65 (br, 1H, Ar, a + b), 7.52 (br, 1H, Ar, a + b), 5.62 (br d, 1H, ²*J*_{PH} = 210, PH, a), 5.31 (br d, 1H, ²*J*_{PH} = 206, PH, b), 2.85 (br m, 1H of a + 1H of b, CH), 2.50–1.00 (br m, 48H of a + 48H of b of dcpce + 3H of a + 3H of b of CH(*Me*)CN), 2.03, 1.92, 1.85 (all br, 18H of a + 18H of b, *o*-*t*-Bu), 1.42 (9H of a + 9H of b, *p*-*t*-Bu).

Pt(dcpce)[CH(Me)(CN)][P(Me)Ph] (14). A white suspension of 150 mg (0.2 mmol) of Pt(dcpce)[CH(Me)(CN)](Br) in 10 mL of THF was treated with 10 mL of a yellow THF solution of freshly prepared NaP(Me)Ph (0.4 mmol), formed by reaction of 73.2 mg (0.4 mmol) of NaN(SiMe₃)₂ and 49.5 mg (0.4 mmol) of PH(Me)(Ph). The suspension became yellow, and it was stirred at room temperature for 2 h. The solvent was then removed in vacuo, and the yellow-orange solid residue was extracted with ca. 20 mL of toluene. The toluene extract was filtered through Celite, the toluene was removed in vacuo, and addition of an excess of petroleum ether to the viscous residue precipitated a yellow solid. This was separated, washed three times with ca. 5 mL of petroleum ether, and dried in vacuo. The solid was then dissolved in ca. 5 mL of toluene, and the resulting solution was passed down a column of Silica gel 60 (ca. 5 mm in height, as well as in diameter). Removal of toluene in vacuo from the eluent gave a yellow microcrystalline solid, which was washed with ca. 2 × 5 mL of petroleum ether and finally dried in vacuo (yield: 80 mg, 50%). NMR showed this material was a mixture of two diastereomers, a and b.

¹H NMR (22 °C, C₆D₆): δ 7.78, 7.60, 7.22 and 7.02 (all m, 5H of a + 5H of b, Ar), 2.85–0.80 (br m, 52 H (dcpce + CH(*Me*)CN) of a + 55 H (dcpce + CH(*Me*)CN + PPh(*Me*) of b), 1.80 (3H, apparent t, ²*J*_{PH} = 6, ⁴*J*_{PH} = 6, ³*J*_{Pt–H} = 49, PPh(*Me*) of a). ¹H NMR (22 °C, THF-*d*₈): δ 7.28, 7.06, 6.88 (all m, 5H of a + 5H of b, Ar), 2.80–0.80 (br m, 55 H (dcpce + CH(*Me*)CN + PPh(*Me*) of a + 55 H (dcpce + CH(*Me*)CN + PPh(*Me*) of b). IR: 2916, 2850, 2185, 1577, 1478, 1446, 1329, 1289, 1273, 1195, 1120, 1040, 1024, 1008, 917, 891, 867, 853, 821, 803, 738, 698, 666, 650, 535, 517, 490. Anal. Calcd for C₃₆H₆₀NP₃Pt: C, 54.40; H, 7.61; N 1.76. Found: C, 54.50; H, 7.85; N, 1.88.

Acknowledgment. We thank the NSF Career Program, the Petroleum Research Fund, administered by the American Chemical Society, the Exxon Education Foundation, DuPont, and Union Carbide (Innovation Recognition Program) for partial support, and Prof. R. P. Hughes for helpful discussions. The University of Delaware thanks the NSF (CHE-9628768) for their support of the purchase of the CCD-based diffractometer.

Supporting Information Available: Details of the crystal structure determinations. This material is available free of charge via the Internet at <http://pubs.acs.org>.

OM9903700